

PROCEEDINGS OF SPIE

[SPIDigitalLibrary.org/conference-proceedings-of-spie](https://spiedigitallibrary.org/conference-proceedings-of-spie)

Evaluation of the initial NOAA AVHRR GAC SST reanalysis version 2 (RAN2 B01)

Pryamitsyn, V., Ignatov, A., Petrenko, B., Jonasson, O.,
Kihai, Y.

V. Pryamitsyn, A. Ignatov, B. Petrenko, O. Jonasson, Y. Kihai, "Evaluation of the initial NOAA AVHRR GAC SST reanalysis version 2 (RAN2 B01)," Proc. SPIE 11420, Ocean Sensing and Monitoring XII, 1142005 (18 May 2020); doi: 10.1117/12.2558751

SPIE.

Event: SPIE Defense + Commercial Sensing, 2020, Online Only

Evaluation of the initial NOAA AVHRR GAC SST Reanalysis Version 2 (RAN2 B01)

V. Pryamitsyn^{*1,2}, A. Ignatov¹, B. Petrenko^{1,2}, O. Jonasson^{1,2}, Y. Kihai^{1,2}

¹NOAA STAR, ²GST, Inc.

ABSTRACT

Under the NOAA AVHRR GAC Reanalysis project (RAN), a global dataset of consistent sea surface temperature (SST) retrievals from 1981-on will be created from multiple NOAA AVHRRs using the ACSPO system. Following release of RAN1 dataset in 2016, the initial RAN2 Beta 01 (“RAN2 B01”) dataset was produced from NOAA-07, 09, 11, 12, 14, 15 and 16 from 1981-2003. This paper evaluates the initial RAN2 B01 dataset and compares it with two other SST datasets, the NOAA-NASA Pathfinder v5.3 (“PF”) and ESA CCI v2.1 (“CCI”). The time series of monthly global biases and standard deviations with respect to uniformly quality controlled *in situ* SSTs, and clear-sky fractions (percent of SST pixels to the total ice-free ocean) are compared. ‘Skin’ and ‘depth’ SSTs, only available in RAN and CCI data sets, and sensitivity of ‘skin’ SST to true SST, are also compared. The RAN B01 outperforms PF. Compared to CCI, it generally delivers more clear-sky observations, often with a better accuracy and precision for both ‘skin’ and ‘depth’ SSTs. The sensitivity to true SST is lower and more variable in RAN2 B01, than in CCI. The RAN2 B01 performance following large volcanic eruptions needs improvements.

1. INTRODUCTION

Data of AVHRR/2s (flown onboard NOAA-07, 09, 11, 12, and 14) and AVHRR/3s (onboard NOAA-15, 16, 17, 18, and 19) instruments, suitable for sea surface temperature (SST) retrievals from bands 3b, 4 and 5 centered at 3.7, 10.8 and 12 μm , have been available from multiple NOAA satellites since September 1981. They allow creation of long-term global SST record [1-6]. NOAA AVHRR GAC Reanalysis (RAN) project covered a period from 2002-2015 [1]. The ongoing second phase of this project (RAN2) will extend the RAN1 dataset to cover full AVHRR period from 1981-on. NOAA enterprise Advanced Clear-Sky Processor for Oceans (ACSPO) SST system is used in the RANs. At the time of this report, the initial “beta” version of the RAN2 dataset (RAN2 B01) was produced by reprocessing AVHRR GAC data from NOAA-07, 09, 11, 12, 14, 15 and 16 from Sep 1981 – Dec 2003. In this paper, we compare the performance of RAN2 B01 SST with two other available SST data sets for this period: the NOAA-NASA Pathfinder v5.3 (“PF”) [2-4] and ESA Climate Change Initiative v2.1 (“CCI”) [5-6]. The main features of the three datasets are described below. Time series of monthly biases and standard deviations of retrieved SSTs minus *in situ* SSTs from drifting and moored buoys are compared, along with monthly numbers of *in situ* matchups and clear-sky fractions (percent of SST pixels to the total ice-free ocean pixels). The RAN2 B01 SSTs “sub-skin” and CCI “skin” SST products are also compared in terms of estimated sensitivities to true “skin” SST.

1.1 RAN2 B01

The SST retrieval, training and cloud masking algorithms, employed in the operational ACSPO processing systems, are described in [7-10]. The modifications to these algorithms, made during RAN2 B01, are presented in [11]. ACSPO generates two SST products. The first product is Global Regression (GR) SST [8], sensitive to “skin” SST, T_{SKIN} . The GR coefficients are adjusted to zero the global bias between GR SST and T_{IS} over the training global dataset of matchups. Therefore, although the GR SST in ACSPO reproduces variations in T_{SKIN} , it remains anchored to “depth” SST, T_{DEPTH} which is why we denominate the ACSPO GR SST as “sub-skin”, rather than “skin” SST. In this paper, when comparing the RAN2 “sub-skin” SST with PF and CCI “skin” SSTs, we add to the two latter products an average “depth-skin” correction of 0.17 K [12]. The second ACSPO product is Piecewise Regression (PWR) SST [9]. The PWR SST is less sensitive to T_{SKIN} but more precise with respect to *in situ* SST, T_{IS} , which is an equivalent of “depth” SST, T_{DEPTH} [12]. Therefore, the ACSPO PWR SST is considered a proxy for T_{DEPTH} . In this paper, we compare it with “depth” SST reported in CCI. (No “depth” SST is reported in PF.)

ACSPO SST is retrieved in the full AVHRR swath, i.e., within the range of view zenith angles $VZA \sim \pm 68^\circ$. Both RAN2 SST products use regression equations with variable coefficients, renewed daily from matchups of clear-sky

*Email: victor.pryamitsyn@noaa.gov; Phone: +1-301-683-3366

brightness temperatures with *in situ* SSTs from drifting and moored buoys ('D+TM'). Due to insufficient and highly variable number of drifting and moored buoys' measurements at 1980's and early 1990's, we have also included the *in situ* SSTs from ships for the calibration (i.e., calculation of the regression coefficients) of NOAA-07, 09 and 11. The GR coefficients for a given day are calculated from matchups collected within a time window of 1 ± 45 days, centered at a given day. The window size for PWR coefficients is 1 ± 180 days. The NLSST algorithm employed in ACSPO, uses first-guess SST on the right side of the equation [13]. In ACSPO, the first-guess SST, T_0 , is additionally used in the ACSPO Clear-Sky mask (ACSM) [7]. Up until RAN2, the T_0 employed in ACSPO was the global daily Canadian Meteorological Center (CMC) L4 analysis [14], available since September 1991. In RAN2 B01, the CMC SST is used as the "first guess" for those missions, which start after this date, i.e., NOAA-12, 14, 15 and 16. The data of NOAA-07, 09 and 11 are processed using the CCI L4 analysis [5-6], available since September 1981. The GR coefficients were calculated using the constraint set on mean sensitivity of GR SST to T_{SKIN} over the training data set of matchups, $\langle \mu \rangle : \langle \mu \rangle = 0.94$ for day and $\langle \mu \rangle = 0.98$ for night [6, 10]. ACSPO producers recommend users to use pixels with quality level QL=5, only [1]. In ACSPO, QL=5 is assigned to pixels, classified as "clear-sky" by the ACSPO Clear-Sky Mask (ACSM), and only these ACSPO data are evaluated in this study.

1.2 Pathfinder v.5.3 ('PF')

The AVHRR PF is the L3C SST data set is a global, twice-daily (Day and Night) 4km SST produced by the NOAA National Centers for Environmental Information (NCEI) [4]. The L3C SST is generated with retrievals combined from a single instrument into a space-time grid. The PF SST is retrieved within a limited range of VZAs, $55^\circ < VZA < 55^\circ$, with regression equations, using two AVHRR bands 10.8 and 12 μm during both day and night. The regression coefficients are recalculated on a monthly basis for two atmospheric water vapor regimes (dry and medium to moist atmospheres), defined by the brightness temperature difference between AVHRR bands 4 and 5. The PF 'skin' SST is obtained from the retrieved SST (trained against *in situ* SST) by subtracting a "depth-skin" bias of 0.17 K. When comparing the PF 'skin' SST with RAN2 B01 'sub-skin' SST, we have added the 0.17 K back. The PF dataset does not include estimates of T_{DEPTH} , nor does it contain estimated sensitivities to true T_{SKIN} .

1.3 Climate Change Initiative v. 2.1 ('CCI')

The CCI dataset [4, 5] provides retrieved SST in three formats: L2P, L3U and L3C. Also CCI program has created its own L4 analysis. In this paper, we compare RAN2 B01 and CCI L2P SSTs. The CCI L2P dataset includes both 'skin' and 'depth' SSTs. The 'skin' SST is produced with the model-based Optimal Estimation (OE) method [15] whereas the "depth" SST is produced from 'skin' SST based on model considerations [6]. Since the OE for 'skin' SST retrieval does not explicitly use *in situ* SSTs in the retrievals (e.g., for training the regression), the CCI SST is deemed to be largely independent from *in situ* measurements. In reality, a high degree of independence has been achieved for the period since 1995-on, when it was possible to use ATSR-2 and AATSR instruments for AVHRR calibration [6]. Prior to that period, CCI employed *in situ* SSTs as a "calibration" reference on large scales. The 'skin' SST was retrieved from two AVHRR bands 10.8 and 12 μm during day and three bands 3.7, 10.8 and 12 μm at night with the algorithms switched at solar zenith angle $SZA=92.5^\circ$ [16]. As recommended by data producers, we used for comparison the CCI SST pixels with quality levels of 4 and 5. Note that CCI SSTs retrieved at $VZA > 60^\circ$ are assigned lower quality levels ($QL \leq 2$), whereas the twilight zone ($92.5^\circ > SZA > 60^\circ$) have quality levels ≤ 3 [16].

2. EXAMPLE: ONE DAY OF SST RETRIEVALS FROM NOAA14

Fig. 1 shows typical geographical distribution of daytime and nighttime satellite minus CMC L4 SSTs, for the three 'sub-skin' SSTs produced from NOAA-14 on 4 February 1996. (Note that the PF and CCI 'skin' SSTs have been shifted by 0.17 K warm, to facilitate comparisons with RAN2 'sub-skin' SST.) PF SST is not available at $|VZA| > 55^\circ$. CCI SSTs at $|VZA| > 60^\circ$ and in the twilight zones are not shown in Fig.1, because they have $QLs < 4$. RAN2 SST is retrieved in the full swath. Comparison of the warm spots during the daytime in Fig. 1 suggests that all three products capture the diurnal cycle fairly consistently. The coldish areas in the maps during both day and night are likely due to residual cloud. Fig. 1 suggests that the RAN2 product is least subject to cloud leakages. Fig. 2 shows deviations from CMC of the corresponding RAN2 and CCI 'depth' SSTs. No 0.17 K bias correction for CCI 'depth' SST was needed. Comparison of the top panels in Figs. 1 and 2 suggests that RAN2 'depth' SST has fewer residual cloud than the corresponding RAN2 'skin' SST, and fewer warm spots during the daytime. The improved agreement of 'depth' SSTs with the foundation CMC L4 is expected, but this is not the case for CCI.

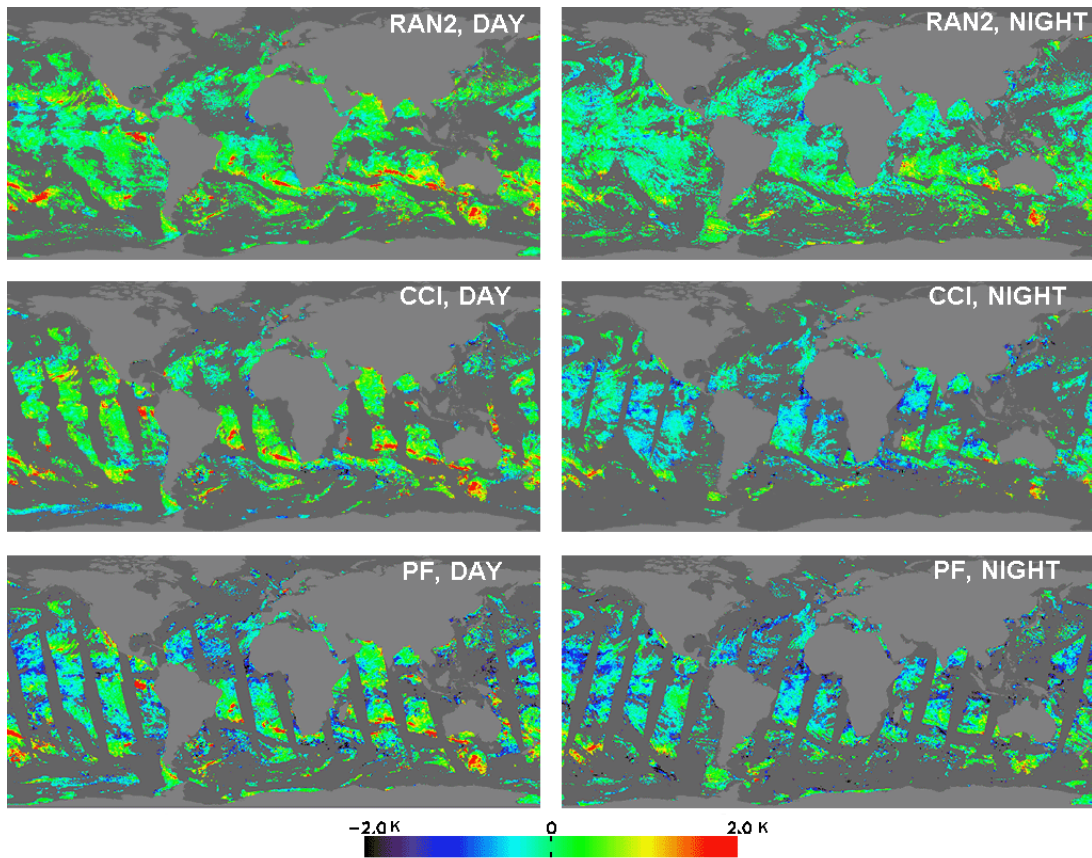


Figure 1. (Left) Daytime and (right) nighttime deviations from CMC of: (top panels) RAN2 B01, (middle panels) CCI v2.1, and (bottom panels) PF v5.3 'sub-skin' SSTs. NOAA-14, 4 February 1996. (CCI and PF SSTs are shifted warm by 0.17 K.)

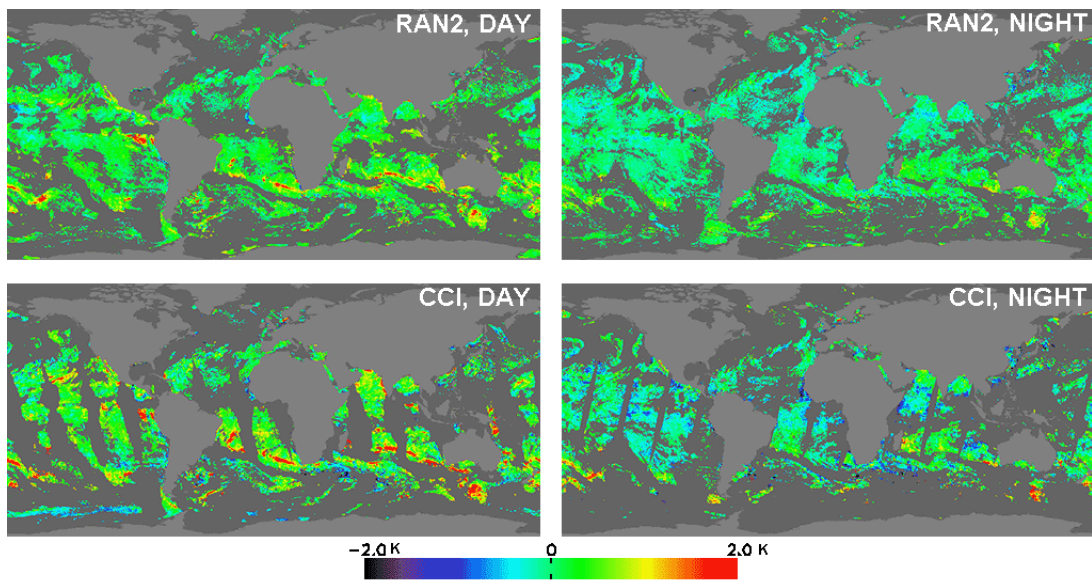


Figure 2. (Left) Daytime and (right) nighttime deviations from CMC of 'depth' SST in (top panels) RAN2 B01 and (bottom panels) CCI v2.1. NOAA-14, 4 February 1996. (Note that no 0.17K bias correction was needed for the CCI 'depth' SST.)

Table 1 shows biases and standard deviations (SDs) of retrieved SST minus *in situ* SST, number of matchups with quality controlled *in situ* data from the NOAA *in situ* SST Quality Monitor (*iQuam*) system [17] (all satellite pixels within $10\text{km} \times 30\text{min}$ window, a standard matchup criteria in the NOAA SST Quality Monitor, SQUAM [18]), and fraction of clear-sky pixels. The precision of PF ‘skin’ SST with respect to *in situ* SST is degraded compared to the two other datasets during day, and comparable with that for CCI at night. The RAN2 B01 produces smallest SDs for ‘skin’ SST during both day and night (in more SST pixels compared to CCI), and these SDs further improve for ‘depth’ SST, as expected. For CCI, the ‘depth’ SDs are comparable to those for ‘skin’, and as a result, the margin between the RAN2 and CCI SDs for ‘depth’ SSTs is wider than for ‘skin’ SSTs.

Table 1. Biases and SDs of RAN2, PF and CCI SSTs with respect to *in situ* SST, numbers of matchups and clear-sky fractions for retrievals from NOAA-14 on 4 February 1996.

Dataset	‘Sub-skin’ SST		‘Depth’ SST		Number of matchups	Clear-Sky Fraction, %
	Bias, K	SD, K	Bias, K	SD (K)		
Day						
PF+0.17 K	-0.12	0.84	N/A	N/A	546	15.6
CCI+0.17 K	-0.08	0.41	+0.03	0.40	560	14.9
RAN2 B01	+0.01	0.39	+0.00	0.32	802	17.4
Night						
PF+0.17 K	-0.27	0.50	N/A	N/A	540	11.3
CCI+0.17 K	-0.35	0.51	-0.17	0.52	856	10.0
RAN2 B01	-0.01	0.41	+0.02	0.37	956	12.1

Fig. 3 shows the geographical distributions of sensitivities of RAN2 ‘sub-skin’ and CCI ‘skin’ SSTs to true T_{SKIN} . The nighttime mean/SD of sensitivity in RAN2 B01 SST are 0.98/0.02, whereas for CCI they are 1.00/0.002. During the day, the numbers are 0.94/0.08 for RAN2 B01 and 0.98/0.02 for CCI. In RAN2 B01, the daytime sensitivity noticeably degrades in the tropics and especially at large VZAs, due to increased water vapor attenuation along the line of sight. At night, the degradation also takes place, but to a much lesser extent. The OE method, used in CCI, allows to always keep the sensitivity very close to its optimal value of 1.

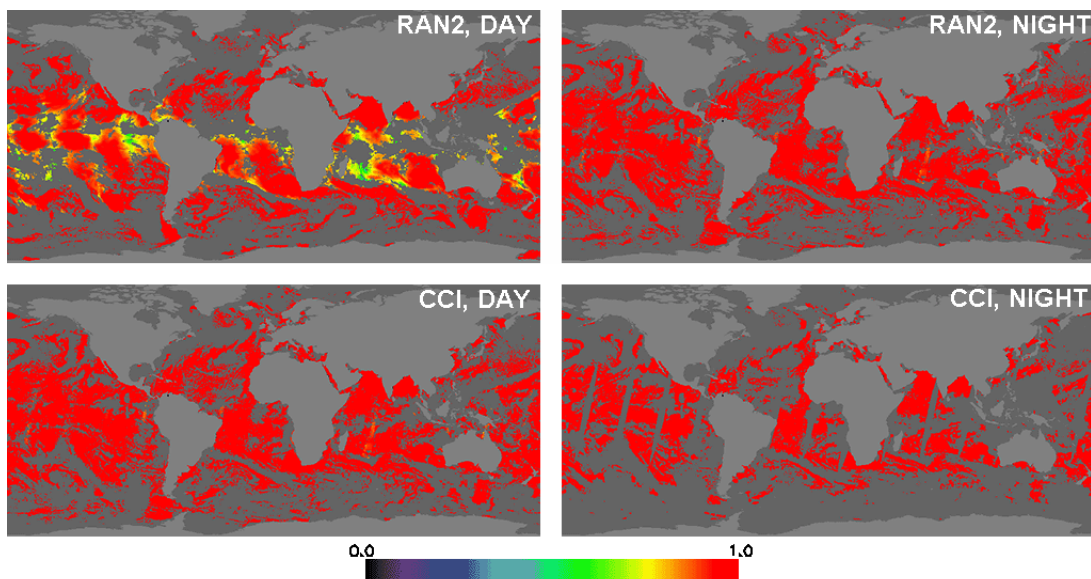


Figure 3. (Left) Daytime and (right) nighttime sensitivities of (top) RAN2 ‘sub-skin’ SST and (bottom) CCI ‘skin’ SST, NOAA14, 4 February 1986.

3. BIASES WITH RESPECT TO *IQUAM IN SITU* SST'S

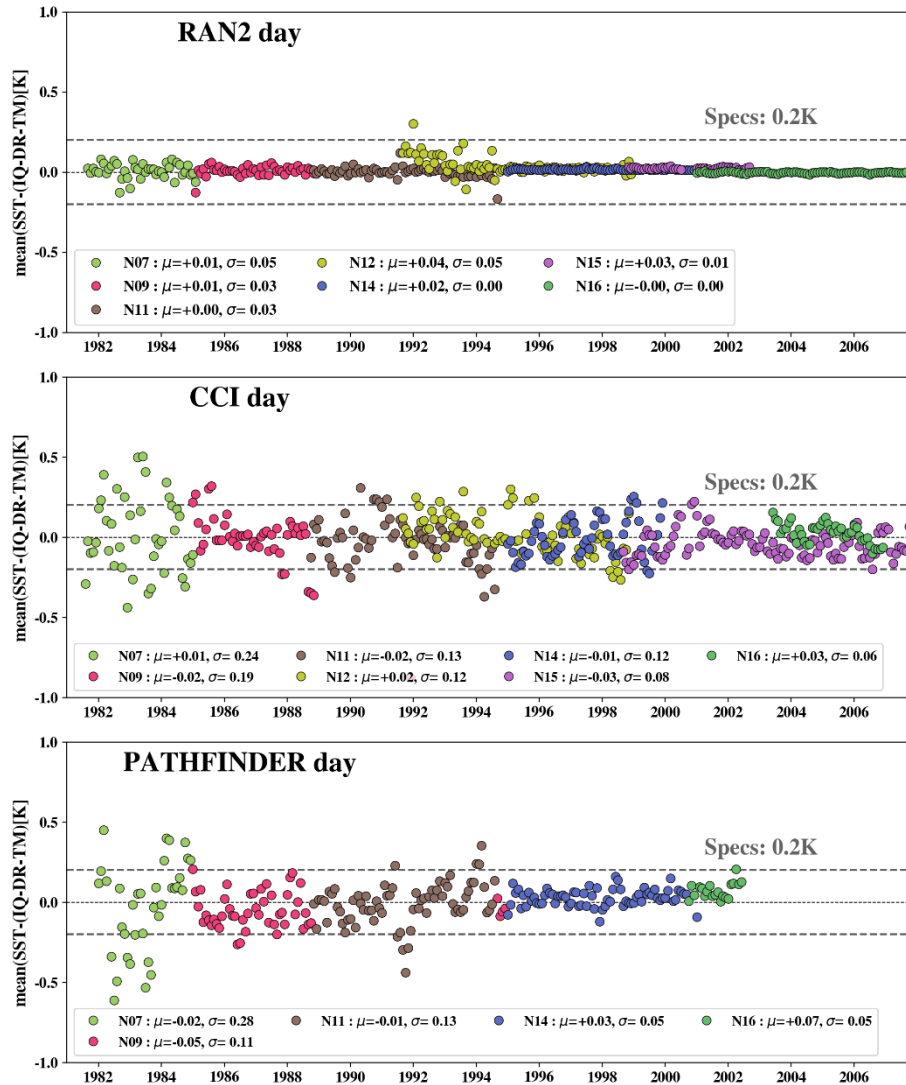


Figure 4. Time series of monthly daytime biases in RAN2 B01, CCI and PF 'sub-skin' SSTs with respect to *iQuam in situ* SSTs. Note that PF does not include data from NOAA-12 and NOAA-15. Recall that both CCI and PF 'skin' SSTs have been shifted warm by 0.17 K, to facilitate comparisons with RAN2 'sub-skin' SST.

Fig. 4 and 5 show time series of monthly mean daytime and nighttime biases in RAN2, CCI and PF 'sub-skin' SSTs with respect to *in situ* SSTs. RAN2 SSTs are tuned to *in situ* SSTs using moving windows (~3 months for GR, and ~6 months for PWR), therefore their biases are expected to be close to zero and stable at all times. Their variations in time (characterized by the respective SDs, also superimposed on the Figures) are all close to zero, with largest SD~0.05 K seen for NOAA-07 and -12 during the day, and 0.07 K for NOAA-7 at night. Note that the PF SSTs are also anchored to *in situ* data monthly, as well as the CCI SSTs prior to 1995, so variable (and negative for PF) biases are somewhat unexpected. The CCI and PF SSTs are less stable, with corresponding SDs reaching 0.24-0.28 K for NOAA-07. Relatively large variations in 'sub-skin' SST from NOAA-07 in all datasets are caused by its unstable AVHRR, and by insufficient and highly variable number of drifting and moored buoys' measurements. These two factors lead to very noisy and uncertain validation, which cannot be improved even by monthly averaging (cf. Figs. 10 and 11 discussed in section 5 below). Relatively high variations in RAN2 'sub-skin' SST from NOAA-12 in mid-1991-1992 are due to the impact of volcanic dust in the atmosphere following two eruptions, of Mt. Pinatubo (Apr-Sep 1991) and Mt. Hudson (Aug 1991). The improvement of the RAN2 SST performance during periods following large volcanic eruptions will be a subject of future work.

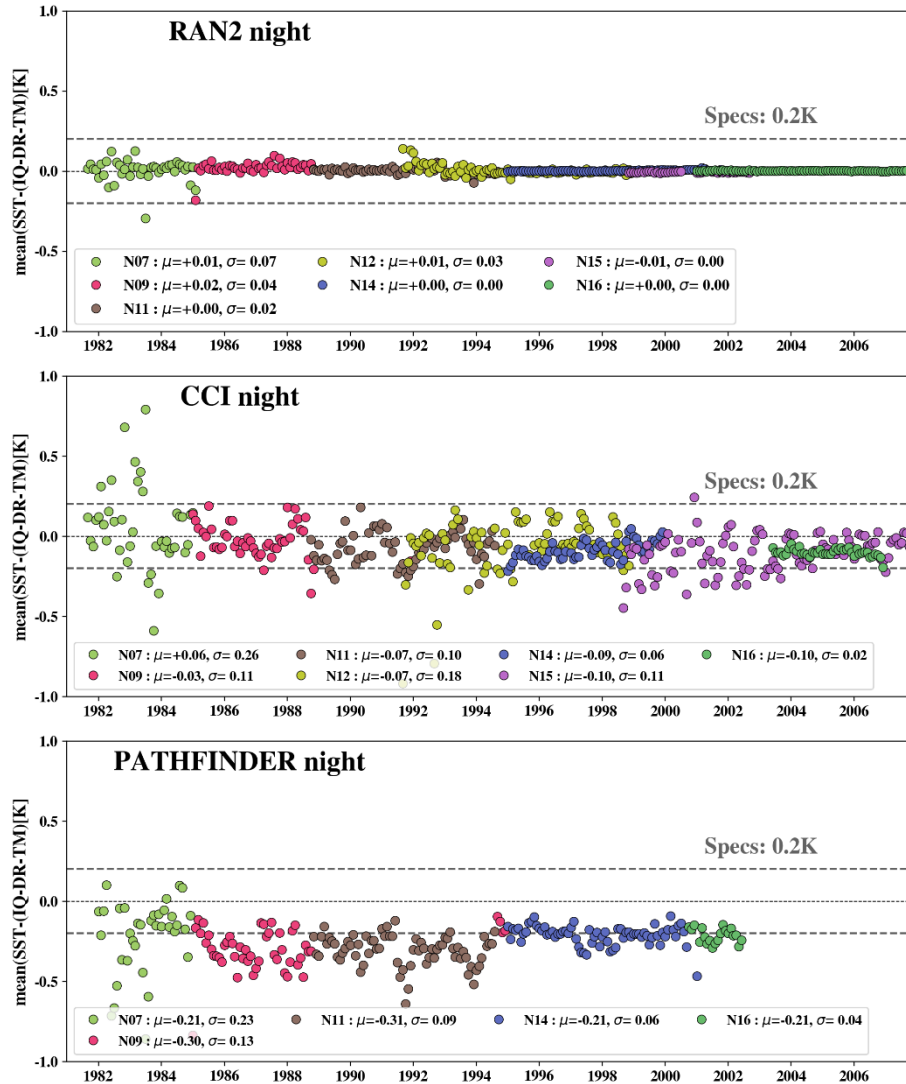


Figure 5. Time series of monthly nighttime biases in RAN2 B01, CCI and PF 'sub-skin' SSTs with respect to *in situ* SSTs.

Fig. 6 shows the time series of monthly biases (both daytime and nighttime) in RAN2 B01 and CCI 'depth' SSTs with respect to *in situ* SST from drifters and tropical moorings. Again, the RAN2 B01 time series are more stable than in CCI. (In fact, the biases in RAN2 B01 'depth' SST are even more stable than in 'sub-skin' SST.) The fact that the SDs of variability in RAN2 B01 biases for NOAA-07 are comparable for 'sub-skin' and 'depth' SSTs suggests that errors of *in situ* data are likely the major contributor to the unstable NOAA-07 SSTs. On the other hand, the SDs of NOAA-12 'depth' SSTs are smaller than those in 'skin' SST, suggesting that the effects of volcanic dust, strongly present in 'sub-skin' SST, are somewhat mitigated in the RAN2 B01 'depth' SST. On the contrary, for CCI the performance statistics of 'depth' SST remain comparable to those for the 'sub-skin' SST, or even slightly degraded.

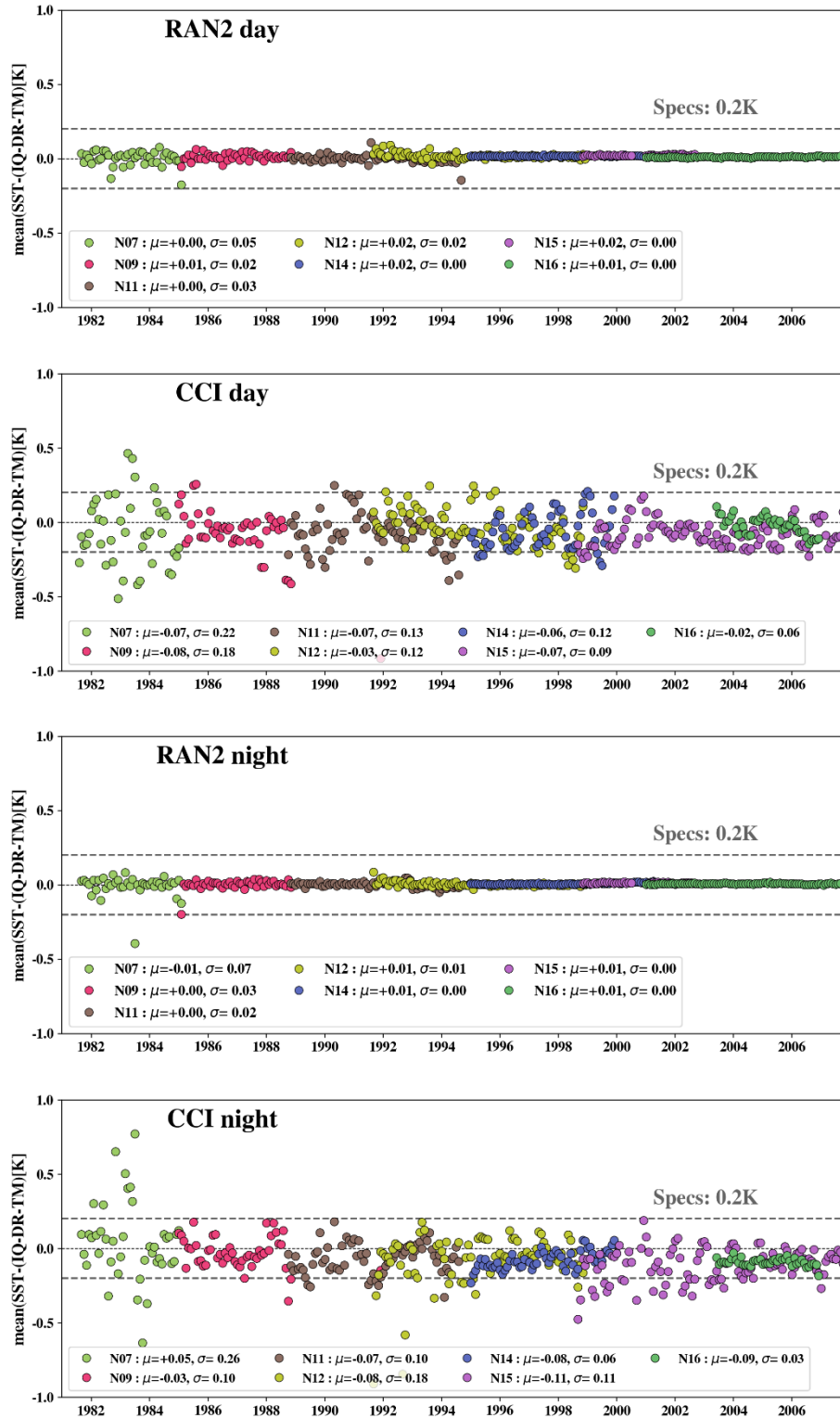


Figure 6. Time series of monthly biases in RAN2 B01 and CCI 'depth' SSTs with respect to in situ SSTs from drifting and moored buoys.

4. STANDARD DEVIATIONS WITH RESPECT TO *IQUAM IN SITU* DATA

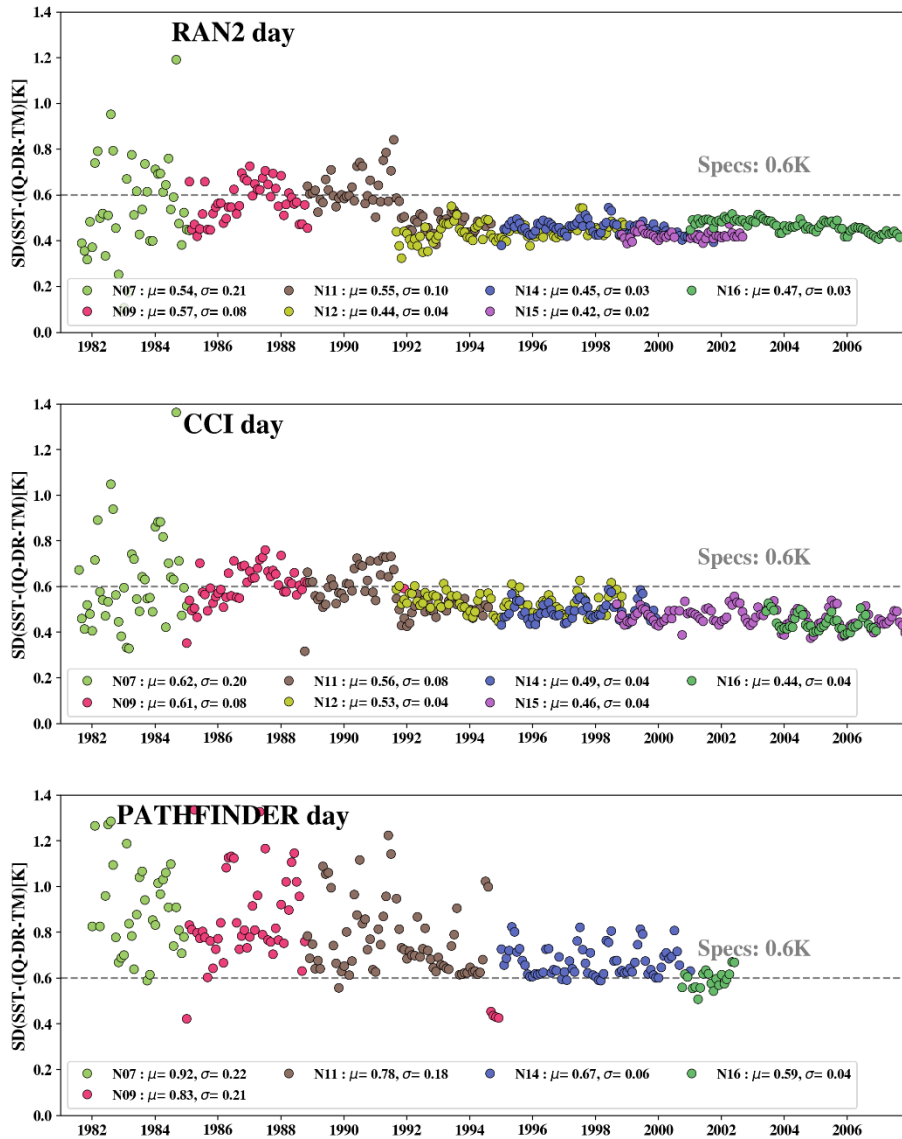


Figure 7. Time series of monthly daytime SDs of RAN2 B01, CCI and PF ‘sub-skin’ SSTs from *iQuam in situ* SSTs.

Figs. 7 and 8 show time series of daytime and nighttime monthly SDs of RAN2 B01, CCI and PF ‘sub-skin’ SSTs with respect to *iQuam in situ* SST, respectively. For almost all satellites, during both day and night, the PF’ SDs are larger than those in RAN2 and CCI (except for NOAA-07 at night, where the SDs of PF and CCI are comparable). SDs in RAN2 B01 are generally smaller than in CCI, for all satellites during day and night, except for NOAA-15 and NOAA-16 during the day. Note that data of NOAA-15 and NOAA-16 are available in CCI and RAN2 B01 for inconsistent periods, and estimated from different time intervals. The comparisons should be repeated after RAN2 is completed, and all data beyond 2003 processed. The increased SDs in RAN2 B01 NOAA-11 ‘sub-skin’ SST in the 1991-1992 is likely due to the impact of volcanic dust from the two eruptions, of Mt. Pinatubo and Mt. Hudson. More work in RAN2 is needed to mitigate those degradations.

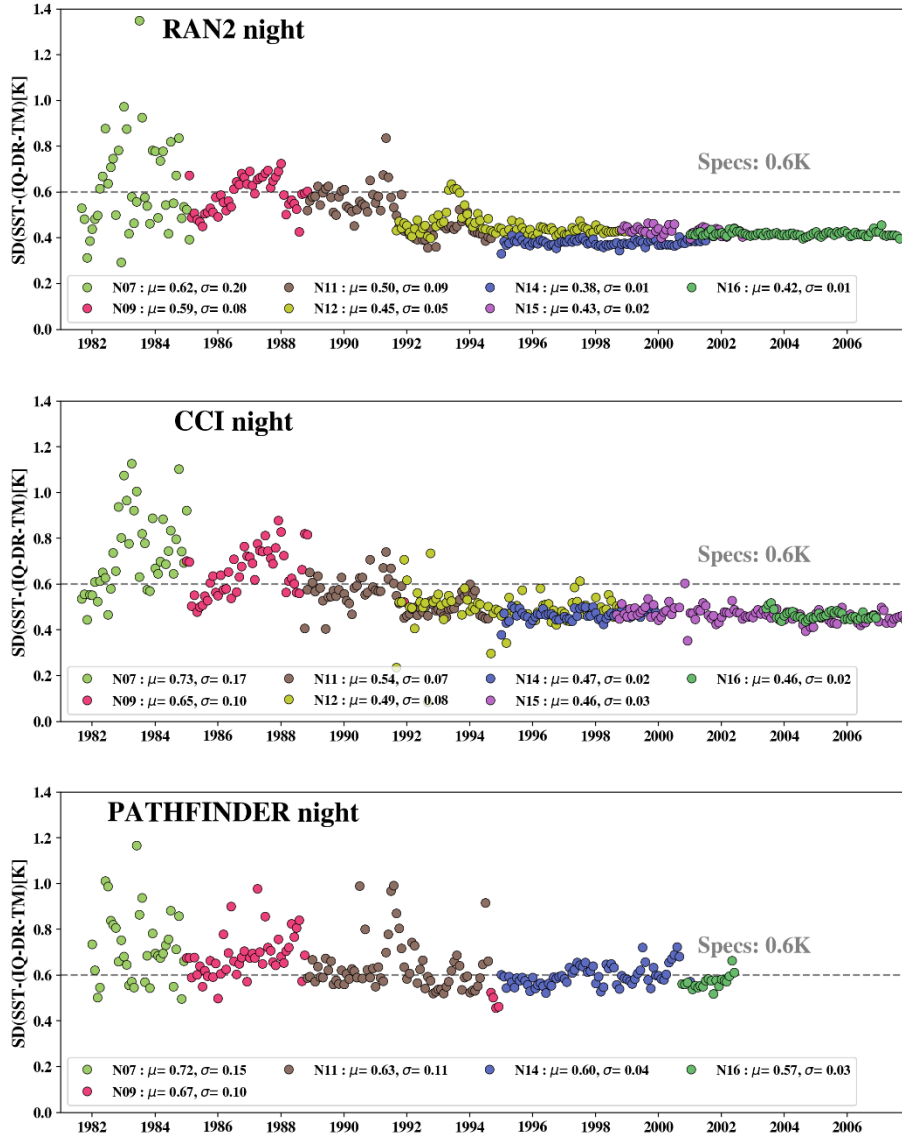


Figure 8. Time series of monthly nighttime SDs of RAN2 B01, CCI and PF 'sub-skin' SSTs with respect to *iQuam* *in situ* SSTs.

Fig. 9 shows time series for daytime and nighttime monthly validation SDs for 'depth' SSTs in RAN2 B01 and CCI SSTs. (Recall that 'depth' SST is not available in PF.) Comparisons with the corresponding plots in Figs. 7 and 8 suggests that in RAN2 B01, 'depth' SST is closer to *in situ* SST than the 'sub-skin' SST, as expected. In contrast, and somewhat counterintuitively, the CCI SDs in 'depth' SST remain comparable to those in 'sub-skin' SST (oftentimes, 'depth' SDs may be even slightly larger than 'skin' SDs; cf. Table 1).

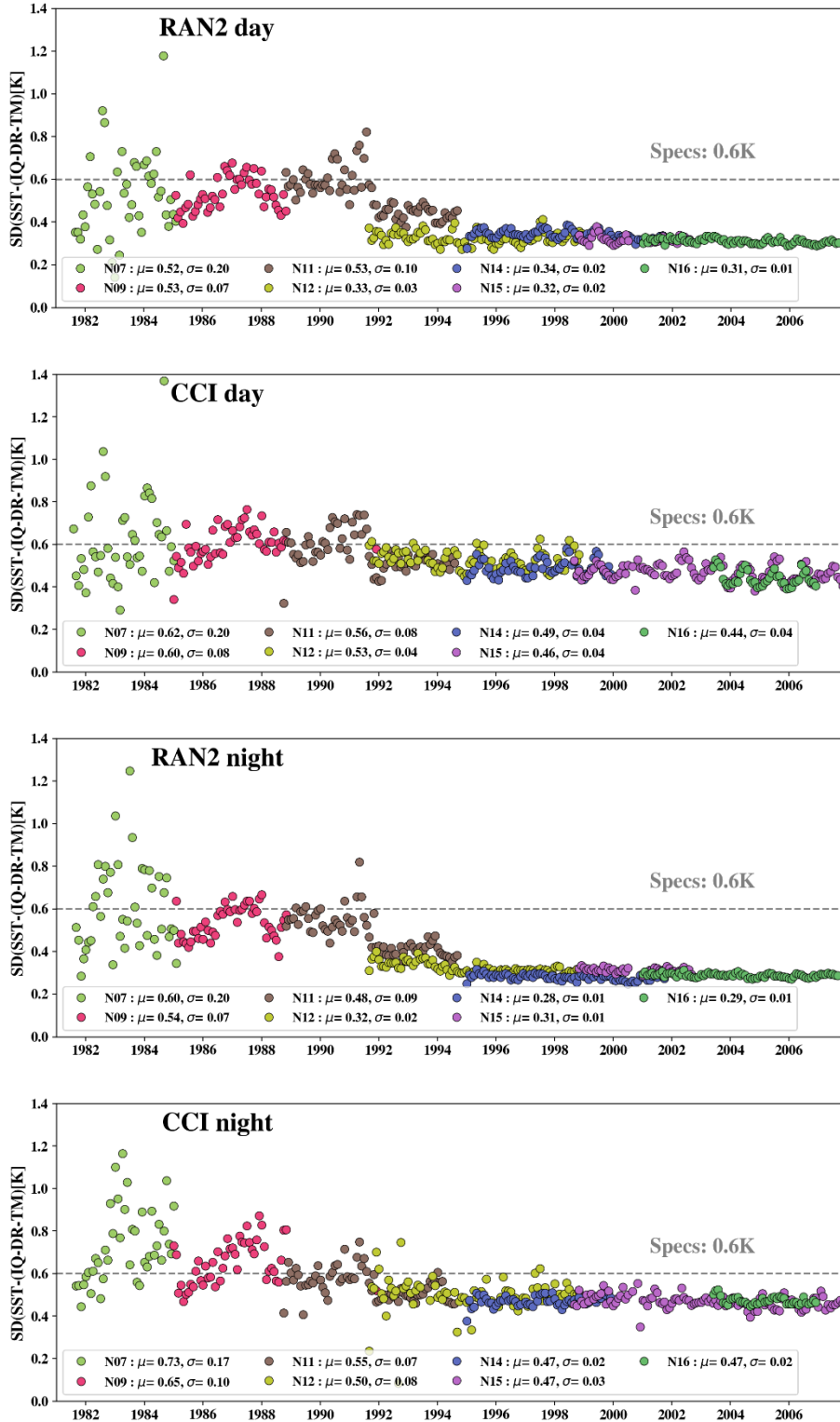


Figure 9. Time series of monthly daytime and nighttime SDs in RAN2 and CCI 'depth' SSTs with respect to iQuam in situ SSTs.

5. NUMBER OF MATCHUPS WITH *IN SITU* AND FRACTION OF CLEAR-SKY PIXELS

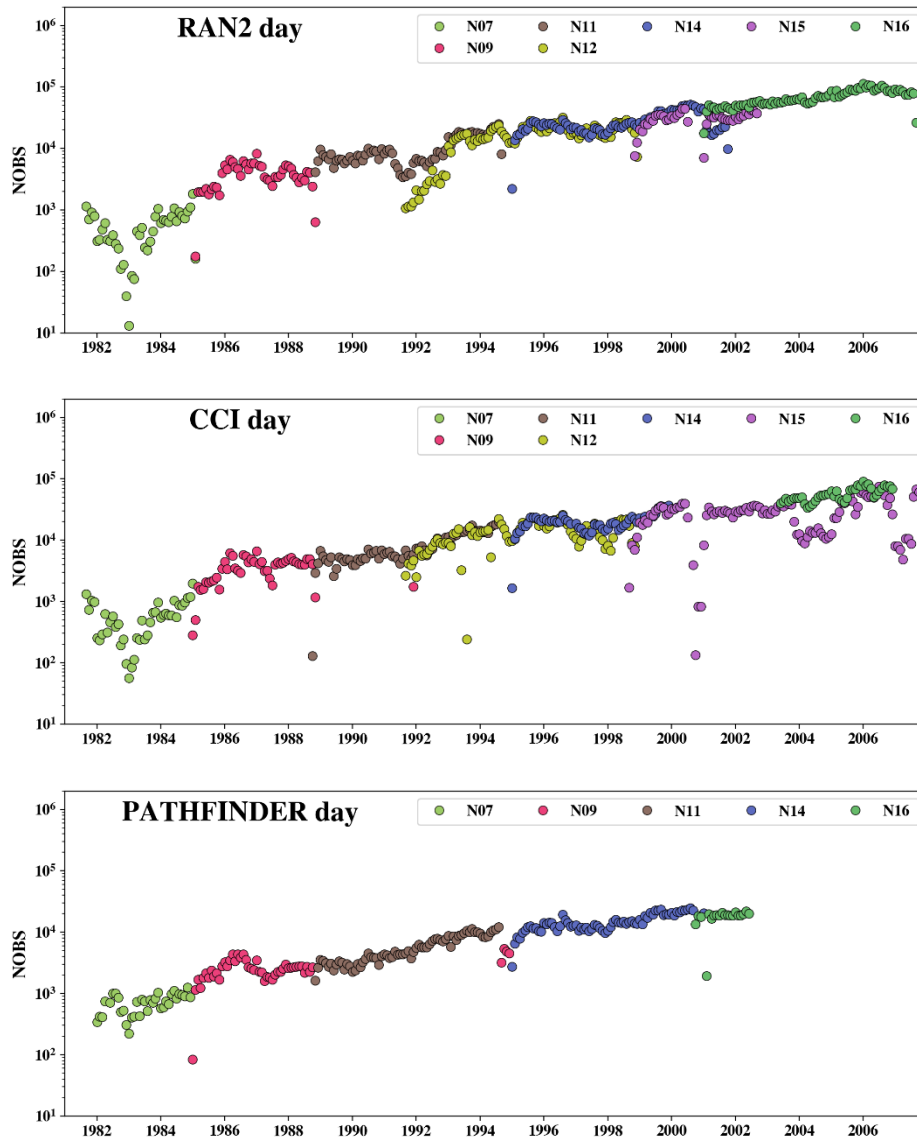


Figure 10. Time series of daytime monthly numbers of matchups with *iQuam in situ* SSTs for RAN2 B01, CCI and PF.

Figs. 10 and 11 show time series of monthly numbers of matchups with drifters and tropical moorings, collected during day- and nighttime in RAN2 B01, CCI and PF (note the logarithmic y-scale). In general, the number of matchups is larger in RAN2 B01 than in CCI and PF. Note also that the PF L3C product may have more satellite retrievals due to collating multiple overpasses, compared to the corresponding RAN2 and CCI L2P products.

Figs. 12 and 13 show daytime and nighttime monthly fractions of quality ocean pixels for RAN2 B01, CCI and PF. Note that comparison of RAN2 B01 and CCI L2P SST products with the PF L3C SST in terms of the clear-sky coverage is not fully consistent. However, we consider the monthly fractions of quality pixels for PF L3C SST as upper estimates of this parameter for the corresponding L2P product. Recall that in RAN2, the quality ocean pixels are identified as pixels with QL=5, which is equivalent to pixels identified as "clear-sky" by the ACSPO Clear-Sky Mask. In CCI, the fraction of quality pixels is composed from pixels with QL=4 and QL=5. Usually, RAN2 B01 provides larger fraction of clear-sky pixels than CCI. One exception is the period from mid' 1991 to 1992, when the number of quality retrievals from NOAA-11 and NOAA-12 in RAN2 B01 are substantially reduced, due to suboptimal processing of the satellite data contaminated with volcanic dust in RAN2 B01.

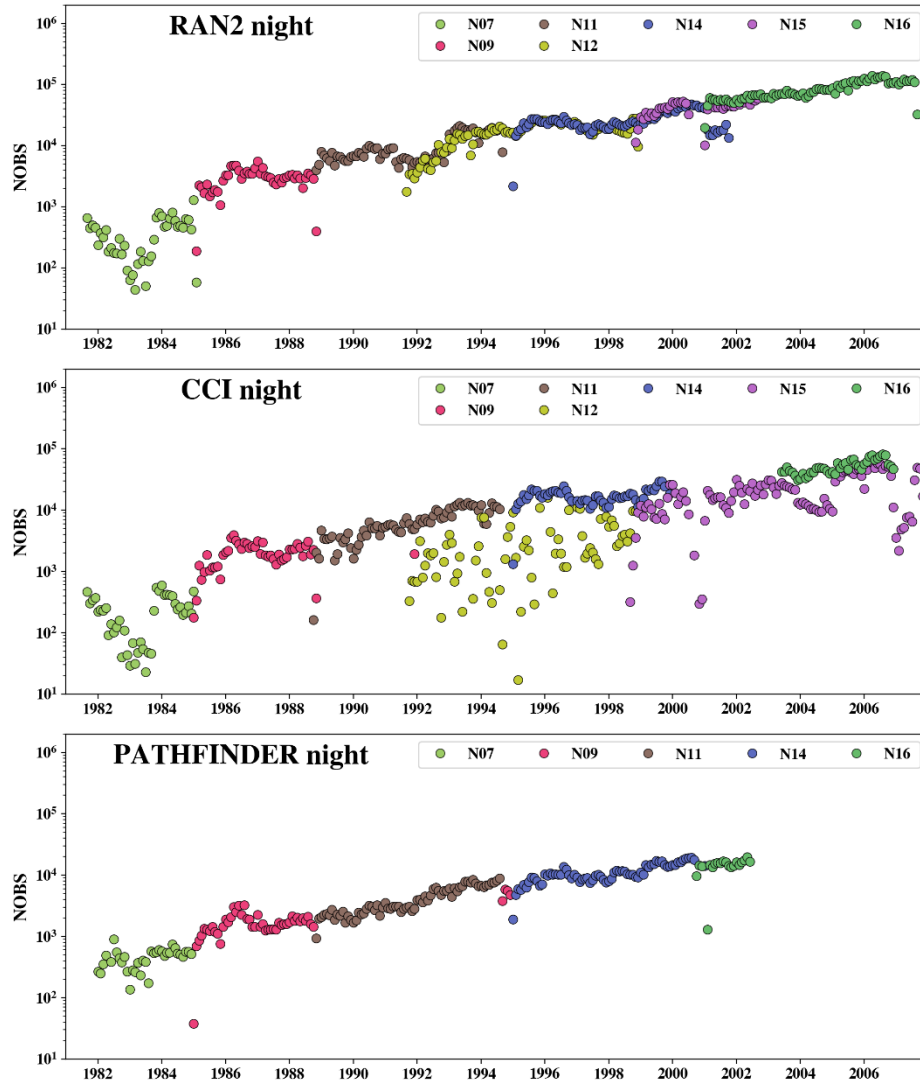


Figure 11. Time series of nighttime monthly numbers of matchups with drifting and moored buoys for RAN2, CCI and PF.

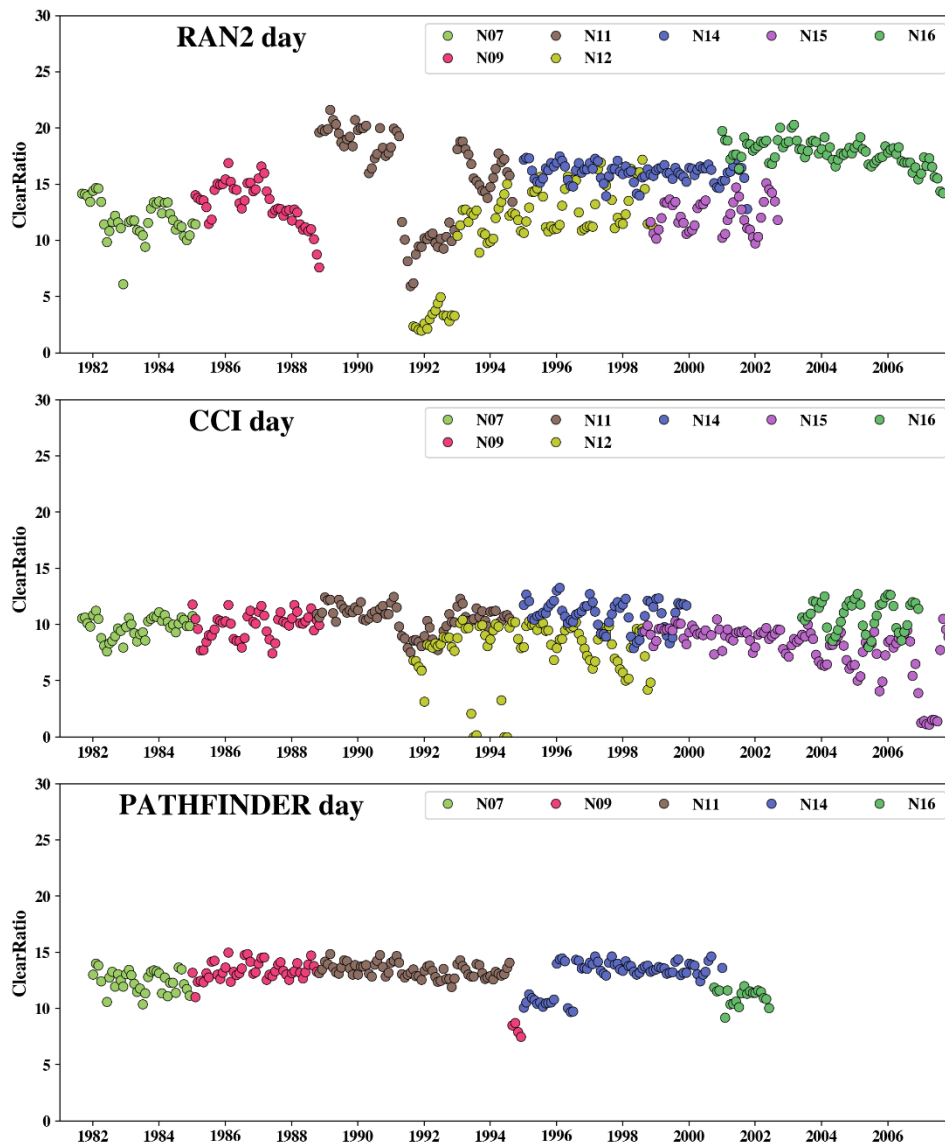


Figure 12. Time series of monthly daytime fractions of quality ocean pixels in RAN2 B01, CCI and PF.

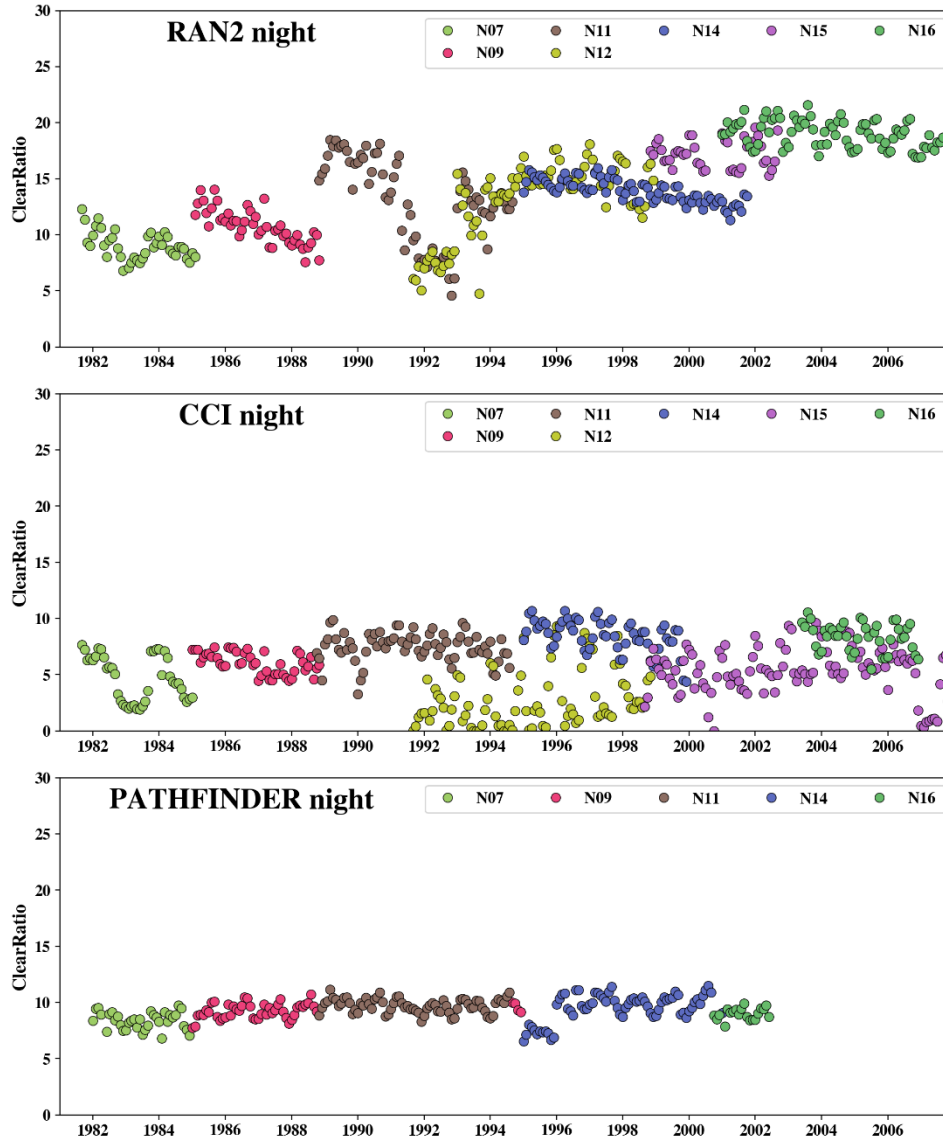


Figure 13. Time series of monthly nighttime fractions of quality ocean pixels in RAN2, CCI and PF.

6. SENSITIVITY TO SKIN SST

Figure 14 shows the time series of monthly daytime and nighttime sensitivities to skin and sub-skin SSTs. For NOAA-09 to NOAA-16, the mean nighttime sensitivities in both RAN2 B01 and CCI are ~ 0.98 , with RAN2 B01 sensitivities being more variable. For NOAA-07 at night, and all satellites during the day, the mean RAN2 B01 sensitivity are 0.92-0.95 (cf. CCI with ~ 1). Analyzes are underway to explore improved sensitivity in RAN2.

7. SUMMARY

The first version of the global RAN2 SST data set (RAN2 B01) from 1981 – 2003 has been created from GAC data of NOAA-07, 09, 11, 12, 14, 15 and 16 with the ACSPO system. Comparison with Pathfinder v5.3 ('PF') and CCI v2.1 ('CCI') has shown the following:

- Accuracy (global mean biases wrt. *in situ* SSTs) and precision (corresponding SDs) of 'skin' SST with respect to *in situ* SST in RAN2 B01 is often comparable to that in CCI, or better. Both RAN2 and CCI outperform the PF.
- In RAN2, 'depth' SST validates better against *in situ* SST compared to 'sub-skin' SST. This is expected. In CCI, the 'skin-depth' margin is narrower and often inverted.

- RAN2 typically provides larger numbers of clear-sky observations than CCI and PF. Exceptions are in mid-1991 to 1992, following two volcanic eruptions, of Mt. Pinatubo and Mt. Hudson.
- SST biases (wrt *in situ* SST) are more stable in RAN2 B01 than in PF and CCI. This is by design of the RAN2 dataset, which is linked to *in situ* data on a rolling bases, and therefore is expected.
- The sensitivity of ‘skin’ SST in RAN2 B01 is on average ~ 0.94 for day and ~ 0.98 for night, whereas in CCI it is very close to the optimum of 1 and less variable.
- The RAN2 B01 SST retrievals are more affected by the volcanic eruptions from mid-1991 to 1992 (NOAA-11 & -12) than CCI SST. Improving RAN2 aerosol correction skill is the subject of future work.

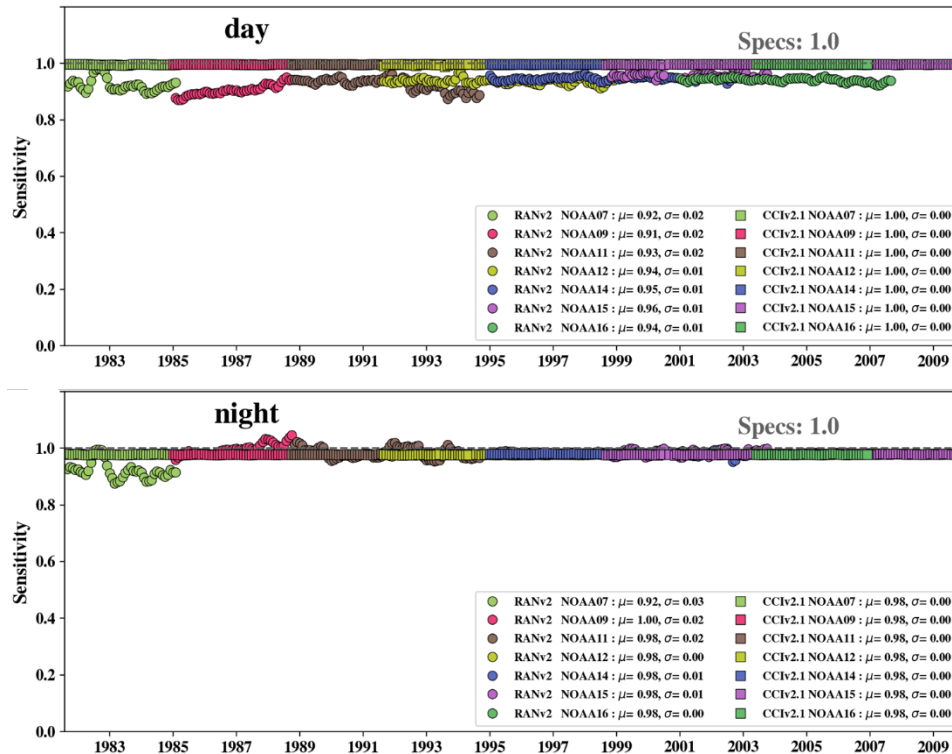


Figure 14. Time series of monthly daytime and nighttime sensitivities to skin SST for CCI and RAN2.

The future work on the AVHRR 2nd Reanalysis (RAN2) will focus on the following tasks:

- Minimizing regional SST biases;
- Improving RAN2 SST performance during 1991-1992, to better mitigate the effects of volcanic dust;
- Testing more efficient filtering of AVHRR sensor issues (by e.g. accounting for sensor temperature & stability);
- Extending the RAN2 dataset to 2018 or longer, as practical;
- Reprocessing RAN2 using the NOAA Geo-Polar Blended (GPB) L4 analysis as the "first guess" as input [19]. The GPB uses RAN data as input, and expected to provide a more consistent first-guess for ACSPO.

8. ACKNOWLEDGEMENT

The views, opinions, and findings in this report are those of the authors and should not be construed as an official NOAA or U.S. government position or policy.

9. REFERENCES

- [1] Ignatov, A., Zhou, X., Petrenko, B., Liang, X., Kihai, Y., Dash, P., Stroup, J., Sapper, J. and DiGiacomo, P., "AVHRR GAC SST Reanalysis Version 1 (RAN1)," *Remote Sens.*, **8**, 315, doi: 10.3390/rs8040315 (2016).
- [2] Kilpatrick, K., Podesta, G., and Evans, R., "Overview of the NOAA/NASA AVHRR Pathfinder algorithm for sea surface temperature and associated matchup database," *JGR*, **106**: 9179-9199 (2001).
- [3] Climate Algorithm Theoretical Basis Document (C-ATBD), Sea Surface Temperature – Pathfinder (2016), www1.ncdc.noaa.gov/pub/data/sds/cdr/CDRs/Sea_Surface_Temperature_Pathfinder/AlgorithmDescription.pdf
- [4] Saha, K., Zhao, X., Zhang, HM, Casey, K., Zhang, D., Baker-Yeboah, S., Kilpatrick, K., Evans, R., Ryan, T., and Relph, J., "AVHRR Pathfinder version 5.3 level 3 collated (L3C) global 4km sea surface temperature for 1981-Present", NOAA NCEI, doi: 10.7289/v52j68xx. Accessed 02 May 2020.
- [5] Merchant, C., Embury, O., and Robert-Jones, J., "Sea surface temperature datasets for climate applications from Phase 1 of the European Space Agency Climate Change Initiative (SST CCI)," *Geoscience Data Journal*, **1**, 179-1991, doi: 10.1002/gdj3.20 (2014).
- [6] Merchant, C., Embury, O., Bugling, C., et al., "Satellite-based time-series of sea-surface temperatures since 1981 for climate applications," *Scientific Data*, **6**:223, doi: 10.1038/s41597-019-0236-x (2019).
- [7] Petrenko, B., Ignatov, A., Kihai, Y., and Heidinger, A., "Clear-sky mask for the Advanced Clear-Sky Processor for Oceans," *JTECH*, **27**, 1609–1623, doi:10/1175/2010JTECHA1413.1 (2010).
- [8] Petrenko, B., Ignatov, A., Kihai, Y., et al., "Evaluation and selection of SST regression algorithms for JPSS VIIRS," *JGR*, **119**, 4580-4599, doi: 10.1117/12.2017454 (2016).
- [9] Petrenko, B., Ignatov, A., Kihai, Y., and Dash, P., "Sensor-Specific Error Statistics for SST in the Advanced Clear-Sky Processor for Oceans," *JTECH*, **33**, 345-359, doi:10.1175/JTECH-D-15-0166.1 (2016).
- [10] Petrenko, B., Ignatov, A., Kramar, M. and Kihai, Y., "Exploring new bands in modified multichannel regression SST algorithms for the next-generation infrared sensors at NOAA," *Proc. SPIE*, **9827**, 9827ON, doi:10.1117/12.2229578 (2016).
- [11] Petrenko, B., Pryamitsyn, V., Ignatov, A., and Kihai, Y., "SST and Cloud Mask Algorithms in Reprocessing 1981-2002 NOAA AVHRR Data for SST with the Advanced Clear-Sky Processor for Oceans (ACSPO)," *Proc. SPIE*, Anaheim, 26-30 April 2020.
- [12] Donlon, C., Robinson, I., Casey, K. et al. "The Global Ocean Data Assimilation Experiment High-Resolution Sea Surface Temperature Pilot Project," *BAMS*, 1197-1213, doi: 10.1175/BAMS-88-8-1197 (2007).
- [13] Walton, C., Pichel, W., Sapper, J., and May, D., "The development and operational application of nonlinear algorithms for the sea surface temperatures with the NOAA polar-orbiting environmental satellites," *JGR*, **103**, 27,999–28,012, doi: 10.1029/98JC02370 (1998).
- [14] Brasnett, B., and Surcel Colan, D., "Assimilating retrievals of sea surface temperature from VIIRS and AMSR2," *JTECH*, **33**, 361-375, doi:10.1175/JTECH-D-15-0093.1 (2016).
- [15] Merchant, C., Le Borgne, P., Roquet, H. and Legendre, G., "Extended optimal estimation techniques for sea surface temperature from the Spinning Enhanced Visible and Infra-Red Imager (SEVIRI)," *Remote Sens. Environ.*, **131**, 287–297, doi:10.1016/j.rse.2012.12.019 (2013).
- [16] Merchant, C. J., Personal communication (13 February 2020).
- [17] Xu, F., and Ignatov, A., "In situ SST Quality Monitor (iQuam)", *JTECH*, **31**, 164-180, doi: 10.1175/JTECH-D-13-00121.1 (2014).
- [18] Dash, P., Ignatov, A., Kihai, Y., Sapper, J., "The SST Quality Monitor (SQUAM)," *JTECH*, **27**, 1899-1917, doi: 10.1175/2010JTECHO756.1 (2010).
- [19] Maturi, E., Harris, A., Mittaz J. et al., "A New High-Resolution Sea Surface Temperature Blended Analysis," *BAMS*, 1015-1026, doi:10.1175/BAMS-D-15-00002.1 (2017).